Numerical solution for Falkner-Skan boundary layer flow of nanofluid

by

Fatima Zulfiqar

A dissertation submitted in partial fulfillment of the requirements
for the degree of Master of Philosophy in Mathematics
Supervised by

Dr. Meraj Mustafa Hashmi

School of Natural Sciences
National University of Sciences and Technology
Islamabad, Pakistan

February 2015

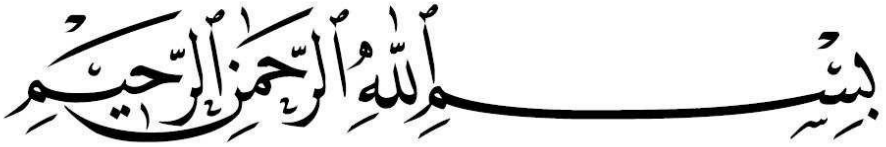

In the Name of Allāh, the Most Gracious, the Most Merciful

Dedicated

To

My Loving Father

Acknowledgment

First and foremost I start with the name of Almighty ALLAH who is the most superior authority. By the grace of ALLAH and HAZRAT MOHAMMAD (S.A.W), I have been able to complete my thesis. Now above all, I wish to express my deepest gratitude to my supervisor, Dr. Meraj Mustafa Hashmi for his guidance, advice and encouragement throughout the preparation of this dissertation. I would also like to thank the GEC members Dr. Yousaf Habib (SNS), Dr. Asif Farooq (SNS) and Dr. Adnan Maqsood (RCMS). Furthermore, I would like to thank my friends and all those who have assisted me directly or indirectly towards the completion of this dissertation specially Mr. Junaid and Mr. Ammar (RCMS).

Finally, I would like to express my extreme gratitude and thanks to my parents. Without their encouragement and support, I can never be at this stage of life. It was my father's utmost desire which took me towards the completion of this degree. I also pay thanks to my family members including my elder brother, sisters, brothers-in-law and sister-in-law. Without their moral support and care, it would have been impossible for me to finish this work.

Abstract

This dissertation deals with the Falkner-Skan flow of nanofluid. The analysis is performed through the revised model for nanofluid which requires nanoparticle volume fraction at the wall to be passively rather than actively controlled. Similarity transformations are used to convert the boundary layer equations into self-similar forms. The numerical solutions of the resulting non-linear ODEs are obtained by an implicit finite difference scheme known as Keller-box method. Graphs are drawn for the influence of various parameters entering in the problem. The obtained numerical results are found in excellent agreement with the previous studies in the limiting cases. .

Preface

The arrangement of the dissertation is as follows:

Chapter 1 is introductory in nature which contains the literature review. It presents some fundamental concepts and the governing laws along with the boundary layer equations. Some details about Keller-box method are also part of this chapter.

Chapter 2 is the review work of Khan and Pop, (Math. Prob. Eng. (2013) doi:10.1155/2013/637825). It is concerned with the boundary layer flow of an impermeable stretching wedge moving in a nanofluid. The developed mathematical problems have been solved by Keller-box method. The physics of the problem is discussed by presenting graphical and numerical results.

Chapter 3 extends the work of Chapter 2 for the newly proposed condition of nanoparticle volume fraction at the wedge. The problems are solved by Keller-box approach and the underlying physics of the problem is thoroughly emphasized.

Contents

Chapter 1

Introduction

In this chapter, the key terminologies pertaining to fluid flow and heat transfer are included. The thermophysical properties of nanofluids are highlighted and compared with those of the conventional base fluids. Applications of nanofluids are also emphasized. The methodology of solution used in the subsequent chapters is thoroughly explained.

1.1 Background

The boundary-layer flow over a moving continuous solid surface is important in many industrial processes. Falkner and Skan [1] were the first to address the steady boundary layer flow past a fixed wedge which enlightened the application of classical Prandtl's boundary layer theory. Falkner-Skan flow problem involves a free stream velocity $U_e = cx^m$, where x is the distance measured along the wall of the wedge. A theoretical study of hydrodynamic and thermal boundary layers resulting from an impulsive Falkner-Skan flow is presented by Harris et al. [2]. In another paper, Pantokratoras [3] presented the effect of variable viscosity on the classical Falkner–Skan flow. The results are obtained with the direct numerical solution of the boundary layer equations. Kuo [4] used the differential transformation method to investigate the temperature field associated with the Falkner–Skan boundary layer problem. An exact analytical solution of the Falkner-Skan equation with mass transfer and wall stretching was derived by Fang

and Zhang [5]. Barania et al. [6] computed series solution of the Falkner-Skan flow problem by homotopy analysis method (HAM). Later, Riley and Weidman [7] and Ishak et al. [8] discussed the multiplicity of solutions for Falkner-Skan flow problem.

Heat transfer has pivotal role in several engineering and biomedical problems. Heat transfer performance of conventional coolants is not appreciable, whereas thermal conductivity of metals is higher when compared with the liquids. The term nanofluid was first used by Choi [9] to refer to the fluids containing nanoparticles. It was observed that thermal conductivity of nanofluids is higher than that of the regular fluids.

Buongiorno [10] presented a mathematical model to study the convective transport in nanofluids. The Cheng–Minkowycz problem for natural convective boundary-layer flow in a porous medium saturated by a nanofluid was discussed by Nield and Kuznetsov [11-12]. They used Buongiorno's model to explore the effects of Brownian motion and thermophoretic diffusion of nanoparticles. In this study the Darcy model was employed for the momentum equation. Simulations were performed through the assumptions of constant wall temperature and constant wall nanoparticle volume fraction. The obtained solution was dependent on four parameters namely the Lewis number Le, the Brownian motion parameter N_B, the buoyancy-ratio parameter Nr, and the thermophoresis parameter N_t.

Similarly Ahmad and Pop [13] investigated the mixed convection from a vertical flat plate embedded in a porous medium filled with nanofluids. In another article, the steady boundary-layer flow of nanofluid past a moving semi-infinite flat plate in a uniform free stream was studied by Bachok et al. [14]. The governing differential system was solved by using the Keller-box approach. Results were obtained for the skin-friction coefficient, the local Nusselt number and the local Sherwood number as well as for the velocity, temperature and the nanoparticle volume fraction profiles.

Another important paper by Khan and Pop [15] discussed the boundary-layer flow of nanofluid induced by a stretching surface. Buongiorno's model was followed in the problem formulation. They investigated the variation of the reduced Nusselt number and the reduced Sherwood number with the variation of embedded parameters. They concluded that reduced Nusselt number is a decreasing function of both Brownian motion and thermophoresis parameters.

Kuznetsov and Nield [16] considered the double-diffusive natural convective boundary layer flow of a nanofluid past a vertical plate. They found that the reduced Nusselt number has inverse relationship with both the thermophoresis parameter and the Brownian motion parameter. In another article, Nield and Kuznetsov [17] discussed the Cheng–Minkowycz problem for the double-diffusive natural convective boundary layer flow in a porous medium saturated by nanofluid.

The boundary layer flow of a nanofluid past a stretching sheet with a convective boundary condition was investigated by Makinde and Aziz [18]. They concluded that strong convective heating at the surface enhances the temperature and heat flux from the plate. In another important article Aziz and Khan [19] examined the natural convective boundary layer flow of nanofluid past a convectively heated vertical plate. Bachok et al. [20] examined the boundary layer flow over a moving surface in nanofluid with suction/injection.

Rana and Bhargava [21] conducted a numerical study on flow and heat transfer of nanofluid above a nonlinearly stretching sheet by finite element method. Bachok et al. [22] studied the boundary layer stagnation-point flow and heat transfer over an exponentially stretching/shrinking sheet in a nanofluid. Zaimi et al. [23] explored the boundary layer flow and heat transfer past a permeable shrinking radiative sheet in a nanofluid. Rahman and El-Tayeb [24] described the radiative heat transfer in the hydro-magnetic nanofluid flow past a non-linear stretching surface considering convective boundary condition.

1.2 Boundary layer

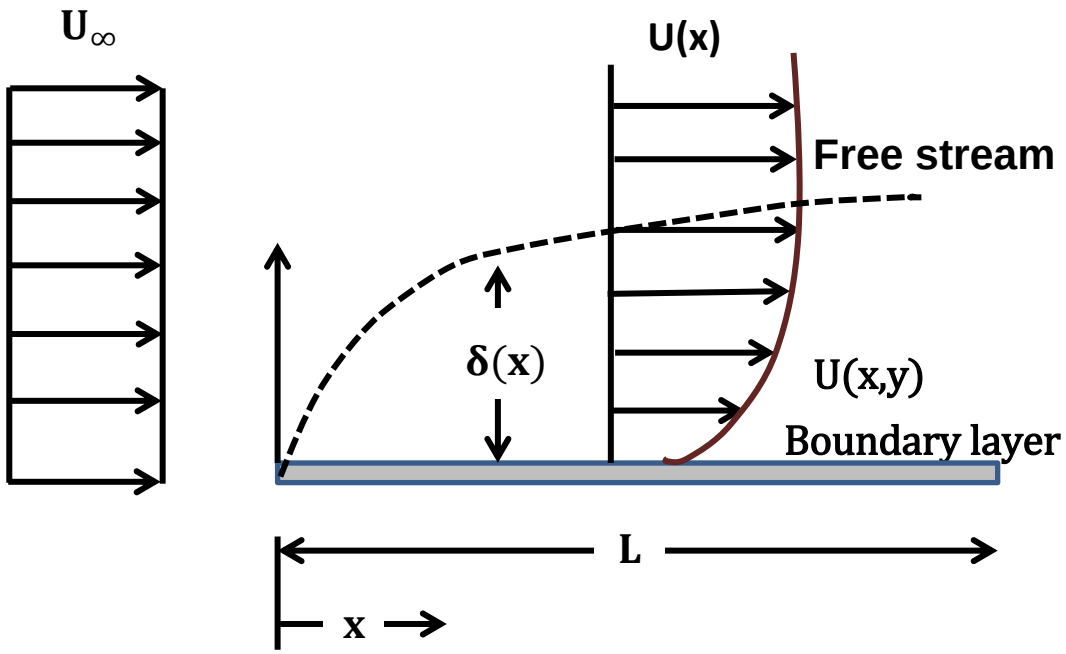

Fig. 1: Boundary layer

Boundary layer is the layer of reduced velocity in fluids, (such as air and water) which is immediately adjacent to the surface of a solid past which the fluid is flowing.

Ludwig Prandtl (1874-1953) is accredited primarily to introduce the concept of boundary layer in fluid flow over a surface. His paper on boundary layer formed the basis for future work on skin friction, heat transfer and separation. The fluid velocity immediately adjacent to the surface is zero due to viscous effects and the fluid layer next to the surface becomes attached to the surface which formulates the no slip condition. The layers of fluid above the surface are moving; hence shearing takes place between the layers of the fluid. The shear stress acting between the wall and the first moving layer next to it is called the wall shear stress and it is denoted by τ_w. The

thickness of the boundary layer is a function of the ratio between inertial forces and viscous forces, that is, the Reynolds number. At low Reynolds number, the flow is laminar and the viscous forces govern the entire boundary layer, however for high Reynolds number, the inertial forces dominate the boundary layer and fluid becomes turbulent.

There are two types of boundary layers:

1. Hydrodynamic (velocity) boundary layer.
2. Thermal boundary layer.

The hydrodynamic boundary layer is the layer of the fluid from the wall to a point where the flow velocity has essentially reached the 'free stream' velocity. The layer of a liquid or gaseous heat transfer agent between the free stream and a heat-exchange surface is termed as thermal boundary layer. In this layer the temperature of the heat-transfer agent changes from that of the wall to that of the free stream. As the fluid velocity increases from zero at the surface to the mainstream, similarly the temperature changes from that at the wall to that in the free stream. The result is that the fluid temperature adjacent to the wall is assumed to be equal to the surface temperature of the wall at the boundary and is equal to the bulk fluid temperature at some point in the fluid.

1.3 Falkner-Skan flow

Falkner-Skan equations involve non-uniform flow which, when calculated at the wall, takes the form ax^m, where x is the coordinate measured along the wedge wall and a and m are constants. These flows are known as Falkner-Skan flows. We assume that the wedge velocity $u_w(x) = -ax^m$ and the free stream velocity is $u_e(x) = cx^m$, where c is arbitrary constant. At the stretching surface, we assume that the temperature T and nanoparticle concentration C has

constant values T_w and C_w respectively. The ambient value of T is denoted by T_∞ and the ambient value of C is denoted by C_∞, as y tends to infinity.

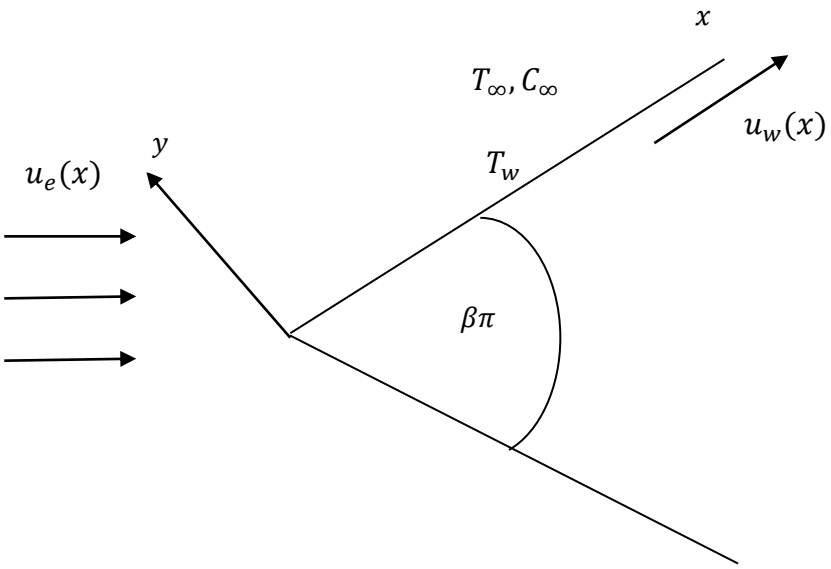

Fig. 2: Schematic diagram of Falkner-Skan flow through a stretching wedge.

Here β denotes the angle which the wedge makes with the horizontal x-axis. $\beta = 0$ corresponds to Blasius flow for a flat plate.

1.4 Nanofluids

Nanofluids are a relatively new class of fluids which consist of base fluid along with suspended nanometer sized particles having diameter less than 100nm. Nanoparticles used in the nanofluids are typically made up of metals (Cu, Ag, Au, Al, Fe), oxide ceramics (Al_2O_3, CuO, TiO_2), nitride ceramics (AlN, SiN), carbide ceramics (SiC, tiC), semiconductors, carbon nanotubes and composite materials such as alloyed nanoparticles. Common base fluids include water, ethylene glycol and oil. It is well known that, conventional heat transfer fluids, such as oil, water, and

ethylene glycol have poor heat transfer properties compared to those of most solids. Nanofluids have enhanced thermophysical properties such as thermal conductivity, thermal diffusivity, viscosity and convective heat transfer coefficients compared with those of base fluids.

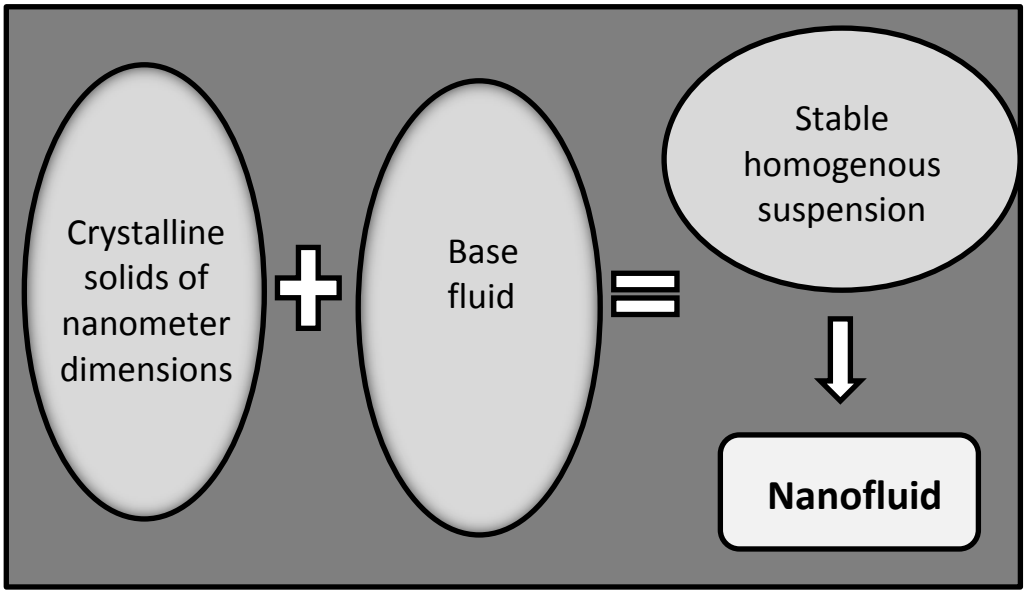

Fig. 3: Nanofluid synthesis

1.4.1 Applications of nanofluids

Nanofluids are useful in many applications in heat transfer including microelectronics, fuel cells, biomedicine, engine cooling, domestic refrigerator, chiller, heat exchanger and the nuclear reactor coolant.

Nanofluids have the four significant features which are desired in the energy systems (fluid and thermal systems). These are:

1. Increased thermal conductivity at low nanoparticle concentration

2. Strong temperature-dependent thermal conductivity
3. Non-linear increase in thermal conductivity with nanoparticle concentration
4. Increase in boiling critical heat flux.

Nanofluids can be used in an excess of technical and biomedical applications such as nanofluid coolant: transformer cooling, computers cooling, electronics cooling, vehicle cooling and electronic devices cooling; medical applications: magnetic drug targeting, cancer therapy and safer surgery by cooling; process industries; materials and chemicals: detergency, food and drink, oil and gas, paper and printing and textiles. Application of nanofluids have various benefits including improved heat transfer, heat transfer system size reduction, minimal clogging, microchannel cooling, and reduction of systems.

1.5 Boundary layer equations for two-dimensional flow of nanofluids

Considering the following assumptions:

1) incompressible flow,
2) no chemical reactions,
3) negligible external forces,
4) dilute mixture,
5) negligible viscous dissipation,
6) negligible radiative heat transfer,
7) nanoparticles and base fluid locally in thermal equilibrium,

the equations governing the conservation of mass, momentum, thermal energy and nanoparticle flux are given by [12].

$$\nabla.\mathbf{V} = 0\,,$$

$$\rho_f\left(\frac{\partial \mathbf{V}}{\partial t} + (\mathbf{V}.\nabla)\mathbf{V}\right) = -\nabla \mathrm{p} + \mu\nabla^2\mathbf{V}\,,$$

$$(\rho c)_f\left(\frac{\partial T}{\partial t} + (\mathbf{V}.\nabla)\mathrm{T}\right) = k\nabla^2 T + (\rho c)_p\left[D_B\nabla C.\nabla T + \left(\frac{D_T}{T_\infty}\right)\nabla T.\nabla T\right], \quad (1.5.1)$$

$$\left(\frac{\partial C}{\partial t} + (\mathbf{V}.\nabla)C\right) = D_B\nabla^2 C + \left(\frac{D_T}{T_\infty}\right)\nabla^2 T\,,$$

in which $\mathbf{V}$ is the velocity field, ρ_f is the density of the base fluid, p is the pressure, ρ_p is the density of the nanoparticle material, T is the temperature, C is nanoparticle concentration, D_B is the Brownian diffusion coefficient and D_T is the thermophoretic diffusion coefficient.

Using the velocity field $\mathbf{V} = [u(x,y),\ v(x,y), 0]$ for two-dimensional flow, temperature field $T = T(x,y)$ and nanoparticle volume fraction $C = C(x,y)$, one obtains:

$$\frac{\partial u}{\partial x} + \frac{\partial v}{\partial y} = 0\,,$$

$$\frac{\partial p}{\partial x} = \mu\frac{\partial^2 u}{\partial y^2} - \rho_f\left(u\frac{\partial u}{\partial x} + v\frac{\partial u}{\partial y}\right), \quad (1.5.2)$$

$$u\frac{\partial T}{\partial x} + v\frac{\partial T}{\partial y} = \alpha\nabla^2 T + \tau\left[D_B\frac{\partial \mathrm{C}}{\partial \mathrm{y}}\frac{\partial T}{\partial y} + \left(\frac{D_T}{T_\infty}\right)\left(\frac{\partial T}{\partial y}\right)^2\right],$$

$$u\frac{\partial C}{\partial x} + v\frac{\partial C}{\partial y} = D_B\frac{\partial^2 C}{\partial \mathrm{y}^2} + \left(\frac{D_T}{T_\infty}\right)\frac{\partial^2 T}{\partial y^2}.$$

1.6 Keller-box method

Most of the problems arising in science and engineering are nonlinear. They are naturally difficult to solve. A very efficient and accurate implicit finite difference method (the Keller box method) can be used for solving nonlinear differential equations. Key characteristics of this method include second order accuracy and unconditional stability.

Keller-box method has the following four main steps:

i. Reduction of the equation or system of equations into a first order system.
ii. Formation of the difference equations using central differences.
iii. Linearization of the resulting algebraic equations (if they are non-linear) by Newton's method.
iv. Solution of the linear system by using block-tridiagonal-elimination procedure.

Chapter 2

Mathematical modeling and analysis for Falkner-Skan flow of nanofluids

This chapter is based on the review of recently published article by Khan and Pop [25]. It deals with the two dimensional incompressible flow of nanofluid over a moving wedge. Section 2.1 is concerned with the mathematical formulation of the problem. Numerical method of solution is described in Section 2.2. Finally the description of results is given in Section 2.3.

2.1 Mathematical formulation of the problem

We consider a two-dimensional incompressible boundary layer flow of nanofluid over an impermeable stretching wedge. Let $u_w(x) = -ax^m$ be the velocity of the stretching wedge and $u_e(x) = cx^m$ be the velocity outside the boundary layer, where a and c are constants. The wedge is maintained at constant temperature T_w. The nanoparticle concentration at the wedge is assumed to be constant i.e. $C = C_w$. The ambient values of T and C are denoted by T_∞ and C_∞.

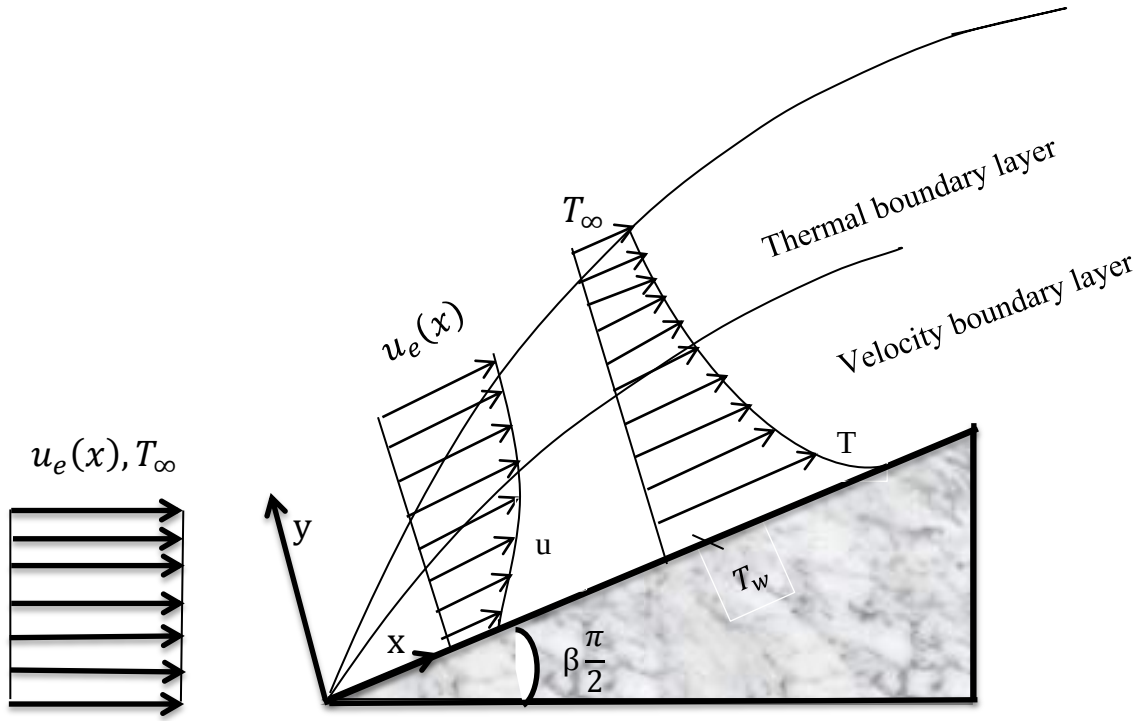

Fig. 4: Velocity and thermal boundary layers for the Falkner-Skan wedge flow.

The boundary layer equations governing the conservation of mass, momentum, thermal energy and nanoparticle concentration are expressed as below:

$$\frac{\partial u}{\partial x} + \frac{\partial v}{\partial y} = 0, \tag{2.1.1}$$

$$u\frac{\partial u}{\partial x} + v\frac{\partial u}{\partial y} = u_e\frac{du_e}{dx} + v\frac{\partial^2 u}{\partial y^2}, \tag{2.1.2}$$

$$u\frac{\partial T}{\partial x} + v\frac{\partial T}{\partial y} = \alpha\frac{\partial^2 T}{\partial y^2} + \tau\left[D_B\frac{\partial C}{\partial y}\frac{\partial T}{\partial y} + \frac{D_T}{T_\infty}\left(\frac{\partial T}{\partial y}\right)^2\right], \tag{2.1.3}$$

$$u\frac{\partial C}{\partial x} + v\frac{\partial C}{\partial y} = D_B\frac{\partial^2 C}{\partial y^2} + \frac{D_T}{T_\infty}\left(\frac{\partial^2 T}{\partial y^2}\right). \tag{2.1.4}$$

The boundary conditions are

$$u = u_w(x) = -\lambda u_e(x), \qquad v = 0, \quad T = T_w, \quad C = C_w \quad \text{at } y = 0,$$
$$u \to u_e(x), \quad T \to T_\infty, \quad C \to C_\infty \quad \text{as } y \to \infty. \tag{2.1.5}$$

[25] Introducing the following dimensionless variables:

$$\eta = \left(\frac{(1+m)u_e}{2xv}\right)^{1/2} y, \quad \psi = \left(\frac{2u_e xv}{1+m}\right)^{\frac{1}{2}} f(\eta), \quad \theta(\eta) = \frac{T-T_\infty}{T_w-T_\infty}, \quad \phi(\eta) = \frac{C-C_\infty}{C_w-C_\infty}. \tag{2.1.6}$$

Eq. (2.1.1) is identically satisfied and Eqs. (2.1.2) – (2.1.5) reduce to the following:

$$f''' + ff'' + \beta(1 - f'^2) = 0, \tag{2.1.7}$$

$$\frac{1}{Pr}\theta'' + f\theta' + N_b\theta'\phi' + N_t\theta'^2 = 0, \tag{2.1.8}$$

$$\phi'' + Lef\phi' + \frac{N_t}{N_b}\theta'' = 0, \tag{2.1.9}$$

subject to the boundary conditions

$$f(0) = 0, \quad f'(0) = -\lambda, \quad \theta(0) = 1, \quad \phi(0) = 1,$$
$$f'(\infty) = 1, \ \ \theta(\infty) = 0, \ \ \phi(\infty) = 0. \tag{2.1.10}$$

Here primes denote differentiation with respect to η. The parameters appearing in Eqs.

(2.1.7)–(2.1.10) are given below:

$$\beta = \frac{2m}{1+m}, \qquad Pr = \frac{v}{\alpha}, \qquad Le = \frac{v}{D_B}, \qquad N_b = \frac{(\rho c)_p D_B (C_W - C_\infty)}{(\rho c)_f v},$$

$$N_t = \frac{(\rho c)_p D_T (T_W - T_\infty)}{(\rho c)_f T_\infty v}. \tag{2.1.11}$$

where β is the measure of pressure gradient, Pr is the Prandtl number, Le is the Lewis number, N_b is the Brownian motion, N_t is the thermophoresis parameter and λ is the ratio of the velocity of the stretching wedge to the free stream velocity. It is important to mention that $\lambda > 0$ corresponds to shrinking wedge whereas $\lambda < 0$ indicates stretching wedge.

The quantities of practical interest are the skin friction coefficient C_f, local Nusselt number Nu and local Sherwood number Sh defined as below:

$$C_f = \frac{\tau_w}{\rho {u_w}^2},$$

$$Nu = \frac{x q_w}{k(T_W - T_\infty)},$$

$$Sh = \frac{x j_w}{D_B (C_W - C_\infty)},$$

using dimensionless variables (2.1.6), one obtains:

$$f''(0) = Re_x^{-1/2} C_f,$$

$$Nur = Re_x^{-1/2} Nu = -\theta'(0),$$

$$Shr = Re_x^{-1/2} Sh = -\phi'(0),$$

where $Re_x = \frac{u_w(x)x}{v}$ is the local Reynold's number and $q_w = -k\left(\frac{\partial T}{\partial y}\right)_{y=0}$ is the wall heat flux.

2.2 Numerical method

The numerical solution for the above coupled ordinary differential Eqs.(2.1.7) - (2.1.9) are obtained using implicit finite difference scheme known as Keller-box method.

2.2.1 Reduction of nth order differential equations to n first order equations

First we introduce new dependent variables $u(\eta)$ and $v(\eta)$such that

$$f' = u, \qquad u' = v, \qquad \theta' = m, \qquad \phi' = n, \tag{2.2.1}$$

so that Eqs.(2.1.7)-(2.1.9) can be written as:

$$v' + fv + \beta(1 - u^2) = 0, \tag{2.2.2}$$

$$\frac{1}{Pr}m' + fm + N_b mn + N_t m^2 = 0, \tag{2.2.3}$$

$$n' + Lefn + \frac{N_t}{N_b}m' = 0. \tag{2.2.4}$$

where primes denote the differentiation with respect to η.

2.2.2 Finite difference discretization scheme

We now consider η as space cordinate and the net points are defined as below:

$$\eta_0 = 0, \qquad \eta_j = \eta_{j-1} + h_j, \qquad j = 1, 2, \ldots . J, \qquad \eta_J = \eta_\infty, \tag{2.2.5}$$

where h_j is the $\Delta\eta$-spacing. Here j is the sequence of numbers that indicate the coordinate location, not tensor indices or exponents.

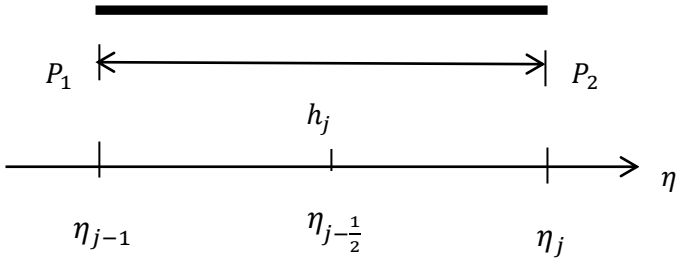

We use the notation $(\,)_{j-\frac{1}{2}}$ for points and quantities midway between net points and for any net function

$$\eta_{j-\frac{1}{2}} = \frac{1}{2}\left(\eta_j + \eta_{j-1}\right). \tag{2.2.6}$$

For any net function u, generally we have:

$$\frac{\partial u}{\partial \eta} = \frac{u_j - u_{j-1}}{k_j}. \tag{2.2.7}$$

We start by writing the finite difference form of Eq. (2.2.1) for the midpoint $(\eta_{j-\frac{1}{2}})$ of the segment P_1P_2 using centered-difference derivatives. This process is called "centering about $(\eta_{j-\frac{1}{2}})$. We get

$$\begin{aligned}
&(f_j - f_{j-1}) - \frac{h_j}{2}(u_j + u_{j-1}) = 0,\\
&(u_j - u_{j-1}) - \frac{h_j}{2}(v_j + v_{j-1}) = 0,\\
&(\theta_j - \theta_{j-1}) - \frac{h_j}{2}(m_j + m_{j-1}) = 0,\\
&(\phi_j - \phi_{j-1}) - \frac{h_j}{2}(n_j + n_{j-1}) = 0,
\end{aligned} \tag{2.2.8}$$

Eqs. (2.2.2)-(2.2.4) are also approximated by centering about $(\eta_{j-\frac{1}{2}})$, we obtain

$$\begin{aligned}
&(v_j - v_{j-1}) + h_j(fv)_{j-\frac{1}{2}} - \beta h_j(u^2)_{j-\frac{1}{2}} + \beta h_j = 0,\\
&\frac{1}{Pr}(m_j - m_{j-1}) + h_j(fm)_{j-\frac{1}{2}} + h_j N_b(nm)_{j-\frac{1}{2}} + h_j N_t(m^2)_{j-\frac{1}{2}} = 0,\\
&(n_j - n_{j-1}) + h_j Le(fn)_{j-\frac{1}{2}} + \frac{N_t}{N_b}(m_j - m_{j-1}) = 0.
\end{aligned} \tag{2.2.9}$$

In terms of new dependent variables, the boundary conditions become:

$$\begin{aligned}
&f(0) = 0, \quad u(0) = -\lambda, \quad u(\infty) = 1, \quad \theta(0) = 1,\\
&\phi(0) = 1, \quad \theta(\infty) = 0, \quad \phi(\infty) = 0.
\end{aligned} \tag{2.2.10}$$

Eq. (2.2.8) is imposed for $j = 1, 2, \ldots J$ at given n, and the transformed boundary layer thickness, η_j, is to be sufficiently large so that it is beyond the edge of the boundary layer. The boundary conditions yield:

$$f_0 = 0, \qquad u_0 = -\lambda, \qquad \theta_0 = 1, \qquad \phi_0 = 1,$$
$$u_J = 1, \qquad \theta_J = \phi_J = 1. \tag{2.2.11}$$

2.2.3 Newton's method

Newton's method is then used to linearize the non-linear system of Eqs.(2.2.8)-(2.2.9). To linearize the nonlinear system of Eqs.(2.2.8)-(2.2.9) using Newton's method, we introduce the following iterate:

$$f_j^{(k+1)} = f_j^{(k)} + \delta f_j^{(k)}, \qquad u_j^{(k+1)} = u_j^{(k)} + \delta u_j^{(k)}, \qquad v_j^{(k+1)} = v_j^{(k)} + \delta v_j^{(k)},$$
$$\theta_j^{(k+1)} = \theta_j^{(k)} + \delta\theta_j^{(k)}, \qquad m_j^{(k+1)} = m_j^{(k)} + \delta m_j^{(k)}, \tag{2.2.12}$$
$$\phi_j^{(k+1)} = \phi_j^{(k)} + \delta\phi_j^{(k)}, \qquad n_j^{(k+1)} = n_j^{(k)} + \delta n_j^{(k)}.$$

Substituting these expressions into Eqs. (2.2.8)-(2.2.9) and then dropping the quadratic and higher-order terms in $\delta f_j^{(k)}, \delta u_j^{(k)}, \delta v_j^{(k)}, \delta\theta_j^{(k)}, \delta m_j^{(k)}, \delta\phi_j^{(k)}, \delta n_j^{(k)}$ yield a linear tridiagonal system.

$$\left(\delta f_j - \delta f_{j-1}\right) - \frac{h_j}{2}\left(\delta u_j + \delta u_{j-1}\right) = (r_1)_j,$$

$$\left(\delta u_j - \delta u_{j-1}\right) - \frac{h_j}{2}\left(\delta v_j + \delta v_{j-1}\right) = (r_2)_j,$$

$$\left(\delta \theta_j - \delta \theta_{j-1}\right) - \frac{h_j}{2}\left(\delta m_j + \delta m_{j-1}\right) = (r_3)_j, \tag{2.2.13}$$

$$\left(\delta \phi_j - \delta \phi_{j-1}\right) - \frac{h_j}{2}\left(\delta n_j + \delta n_{j-1}\right) = (r_4)_j,$$

$$(a_1)_j \delta v_j + (a_2)_j \delta v_{j-1} + (a_3)_j \delta f_j + (a_4)_j \delta f_{j-1} + (a_5)_j \delta u_j = (r_5)_j,$$

$$(b_1)_j \delta m_j + (b_2)_j \delta m_{j-1} + (b_3)_j \delta f_j + (b_4)_j \delta f_{j-1} + (b_5)_j \delta n_j + (b_6)_j \delta n_{j-1} = (r_6)_j,$$

$$(c_1)_j \delta n_j + (c_2)_j \delta n_{j-1} + (c)_j \delta f_j + (c_4)_j \delta f_{j-1} + (c_5)_j \delta m_j + (c_6)_j \delta m_{j-1} = (r_7)_j .$$

where

$$(a_1)_j = 1 + h_j f_{j-\frac{1}{2}}, \quad (a_2)_j = -1 + h_j f_{j-\frac{1}{2}}, \quad (a_3)_j = h_j v_{j-\frac{1}{2}}, \quad (a_4)_j = (a_3)_j . \tag{2.2.14}$$

$$(b_1)_j = \frac{1}{Pr} + \frac{h_j}{2} f_{j-\frac{1}{2}} + h_j N_b \eta_{j-\frac{1}{2}}, \quad (b_2)_j = -\frac{1}{Pr} + \frac{h_j}{2} f_{j-\frac{1}{2}} + h_j N_b \eta_{j-\frac{1}{2}},$$

$$(b_3)_j = \frac{h_j}{2} m_{j-\frac{1}{2}}, \quad (b_4)_j = (b_3)_j, \quad (b_5)_j = h_j \frac{N_b}{2} m_{j-\frac{1}{2}}, \quad (b_6)_j = h_j \frac{N_b}{2} m_{j-\frac{1}{2}}, \tag{2.2.15}$$

$$(c_1)_j = 1 + \frac{h_j}{2} Le f_{j-\frac{1}{2}}, \quad (c_2)_j = -1 + \frac{h_j}{2} Le f_{j-\frac{1}{2}}, \quad (c_3)_j = \frac{h_j}{2} Le \eta_{j-\frac{1}{2}},$$

$$(c_4)_j = \frac{h_j}{2} Le\, \eta_{j-\frac{1}{2}}, \quad (c_5)_j = \frac{N_t}{N_b}, \quad (c_6)_j = -\frac{N_t}{N_b}, \tag{2.2.16}$$

$$(r_1)_j = (f_{j-1} - f_j) + h_j u_{j-\frac{1}{2}}, \qquad (r_2)_j = (u_{j-1} - u_j) + h_j v_{j-\frac{1}{2}},$$

$$(r_3)_j = (\theta_{j-1} - \theta_j) + h_j m_{j-\frac{1}{2}}, \qquad (r_4)_j = (\phi_{j-1} - \phi_j) + h_j n_{j-\frac{1}{2}},$$

$$(r_5)_j = -(v_j - v_{j-1}) - 2h_j f_{j-\frac{1}{2}} v_{j-\frac{1}{2}} + \beta h_j u^2{}_{j-\frac{1}{2}}, \tag{2.2.17}$$

$$(r_6)_j = -\frac{1}{Pr}(m_j - m_{j-1}) - h_j f_{j-\frac{1}{2}} m_{j-\frac{1}{2}} - h_j N_b m_{j-\frac{1}{2}} n_{j-\frac{1}{2}} - h_j N_t m^2{}_{j-\frac{1}{2}},$$

$$(r_7)_j = -(n_j - n_{j-1}) - h_j Le f_{j-\frac{1}{2}} n_{j-\frac{1}{2}} - \frac{N_t}{N_b}(m_j - m_{j-1}).$$

We recall the boundary conditions (2.2.11) to complete the system (2.2.13), which can be satisfied exactly with no iteration. Therefore, for maintaining these correct values in all iterates, we take

$$\delta f_0 = 0, \qquad \delta u_0 = 0, \qquad \delta u_J = 0, \qquad \delta \theta_0 = 0,$$
$$\delta \theta_J = 0, \qquad \delta \phi_0 = 0, \qquad \delta \phi_J = 0. \tag{2.2.18}$$

2.2.4 The block tridiagonal matrix

The linearized difference Eq. (2.2.13) have a block tridiagonal structure consisting of block matrices. The tridiagonal matrix is defined as:

$$[A][\delta] = [r]. \tag{2.2.19}$$

The elements of the matrices are defined as follows:

$$\begin{bmatrix} [A_1] & [C_1] & & & & & \\ [B_2] & [A_2] & [C_2] & & & & \\ & & & \ddots & & & \\ & & & \ddots & & & \\ & & & \ddots & & & \\ & & & & [B_{J-1}] & [A_{J-1}] & [C_{J-1}] \\ & & & & & [B_J] & [A_J] \end{bmatrix} \begin{bmatrix} [\delta_1] \\ [\delta_2] \\ \vdots \\ [\delta_{J-1}] \\ [\delta_J] \end{bmatrix} = \begin{bmatrix} [r_1] \\ [r_2] \\ \vdots \\ [r_{J-1}] \\ [r_J] \end{bmatrix}, \tag{2.2.20}$$

where the elements of the matrices are given as below:

$$[A_1] = \begin{bmatrix} 0 & 0 & 0 & 1 & 0 & 0 & 0 \\ d & 0 & 0 & 0 & d & 0 & 0 \\ 0 & d & 0 & 0 & 0 & d & 0 \\ 0 & 0 & d & 0 & 0 & 0 & d \\ a_2 & a_8 & a_{10} & a_3 & a_1 & a_7 & a_9 \\ b_2 & b_8 & b_{10} & b_3 & b_1 & b_7 & b_9 \\ c_2 & c_8 & c_{10} & c_3 & c_1 & c_7 & c_9 \end{bmatrix} \text{ where } d = -\frac{h_1}{2}, \tag{2.2.21}$$

$$[A_j] = \begin{bmatrix} d & 0 & 0 & 1 & 0 & 0 & 0 \\ -1 & 0 & 0 & 0 & d & 0 & 0 \\ 0 & -1 & 0 & 0 & 0 & d & 0 \\ 0 & 0 & -1 & 0 & 0 & 0 & d \\ a_6 & a_{12} & a_{14} & a_3 & a_1 & a_7 & a_9 \\ b_6 & b_{12} & b_{14} & b_3 & b_1 & b_7 & b_9 \\ c_6 & c_{12} & c_{14} & c_3 & c_1 & c_7 & c_9 \end{bmatrix} \text{ where } d = -\frac{h_j}{2}, \ 2 \le j \le J, \tag{2.2.22}$$

$$[B_j] = \begin{bmatrix} 0 & 0 & 0 & -1 & 0 & 0 & 0 \\ 0 & 0 & 0 & 0 & d & 0 & 0 \\ 0 & 0 & 0 & 0 & 0 & d & 0 \\ 0 & 0 & 0 & 0 & 0 & 0 & d \\ 0 & 0 & 0 & a_4 & a_2 & a_8 & a_{10} \\ 0 & 0 & 0 & b_4 & b_2 & b_8 & b_{10} \\ 0 & 0 & 0 & c_4 & c_2 & c_8 & c_{10} \end{bmatrix} \text{ where } d = -\frac{h_j}{2}, \ 2 \le j \le J, \tag{2.2.23}$$

$$[C_j] = \begin{bmatrix} d & 0 & 0 & 0 & 0 & 0 & 0 \\ 1 & 0 & 0 & 0 & 0 & 0 & 0 \\ 0 & 1 & 0 & 0 & 0 & 0 & 0 \\ 0 & 0 & 1 & 0 & 0 & 0 & 0 \\ a_5 & a_{11} & a_{13} & 0 & 0 & 0 & 0 \\ b_5 & b_{11} & b_{13} & 0 & 0 & 0 & 0 \\ c_5 & c_{11} & c_{13} & 0 & 0 & 0 & 0 \end{bmatrix} \text{ where } d = -\frac{h_j}{2}, \ 1 \le j \le J-1, \tag{2.2.24}$$

$$[\delta_1] = \begin{bmatrix} \delta v_0 \\ \delta m_0 \\ \delta n_0 \\ \delta f_1 \\ \delta u_1 \\ \delta \theta_1 \\ \delta \phi_1 \end{bmatrix}, \qquad [\delta_j] = \begin{bmatrix} \delta u_{j-1} \\ \delta \theta_{j-1} \\ \delta \phi_{j-1} \\ \delta f_j \\ \delta v_j \\ \delta m_j \\ \delta n_j \end{bmatrix};\ 2 \le j \le J\ , \qquad [\mathrm{r_j}] = \begin{bmatrix} (\mathrm{r}_1)_j \\ (\mathrm{r}_2)_j \\ (\mathrm{r}_3)_j \\ (\mathrm{r}_4)_j \\ (\mathrm{r}_5)_j \\ (\mathrm{r}_6)_j \\ (\mathrm{r}_7)_j \end{bmatrix};\ 1 \le j \le J. \tag{2.2.25}$$

(2.2.26)

To solve Eq. (2.2.19), we assume that matrix A is non-singular and it can be factored into

$$[A] = [L][U], \tag{2.2.27}$$

where

$$[L] = \begin{bmatrix} [\alpha_1] & & & & & \\ [\beta_2] & [\alpha_2] & & & & \\ & \ddots & & & & \\ & \ddots & & & & \\ & \ddots & & & & \\ & & [\beta_{J-1}] & [\alpha_{J-1}] & & \\ & & & [\beta_J] & [\alpha_J] \end{bmatrix} \text{ and}$$

$$[U] = \begin{bmatrix} [I_1] & [\Gamma_1] & & & & \\ & [I_2] & [\Gamma_2] & & & \\ & & \ddots & & & \\ & & \ddots & & & \\ & & \ddots & & & \\ & & & [I_{J-1}] & [\Gamma_{J-1}] & \\ & & & & [I_J] \end{bmatrix}, \tag{2.2.28}$$

where $[I]$ is the identity matrix of order 7 and $[\alpha_i]$, and $[\Gamma_i]$ are 7×7 matrices whose elements are determined by the following equations:

$$[\alpha_1] = [A_1], \tag{2.2.29}$$

$$[A_1]\,[\Gamma_1] = [C_1] \text{ and} \tag{2.2.30}$$

$$[\alpha_j] = [A_j] - [B_j][\Gamma_{j-1}],\ \ j = 2,3,\ldots..,J \tag{2.2.31}$$

$$[A_j]\,[\Gamma_j] = [C_j],\quad j = 2,3,\ldots..,J-1. \tag{2.2.32}$$

Now substitute Eq. (2.2.27) into Eq. (2.2.19), to get (2.2.33)

$$[L][U][\delta] = [r]. \tag{2.2.34}$$

Suppose $[U][\delta] = [W]$, (2.2.35)

then Eq. (2.2.33) becomes $[L][W] = [r]$,

where

$$W = \begin{bmatrix} [W_1] \\ [W_2] \\ \vdots \\ [W_{J-1}] \\ [W_J] \end{bmatrix}, \tag{2.2.36}$$

and the $[W_j]$ are 7×1 column matrices. The element W can be solved from Eq. (2.2.35).

$$[\alpha_1]\,[W_1] = [r_1], \tag{2.2.37}$$

$$[\alpha_j]\,[W_j] = [r_j] - [\beta_j][W_{j-1}],\ \ 2 \le j \le J. \tag{2.2.38}$$

These calculations are repeated until convergence criterion is satisfied. Calculations are stopped when

$$\left|\delta n_0{}^{(i)}\right| < \varepsilon, \tag{2.2.39}$$

where ε is small prescribed value.

2.3 Results and discussion

m	Yih [27]	Yacob et al. [28]	White [29]	Present results
0	0.4696	0.4696	0.4696	0.4696001
1/11	0.6550	0.6550	0.6550	0.6549937
1/5	0.8021	0.8021	0.8021	0.8021257
1/3	0.9276	0.9276	0.9277	0.9276809
1/2	-	-	1.0389	1.0389036
1		1.2326	1.2326	1.2325878

Table 2.1: [1] Comparison of the values of $f''(0)$ for different values of *m* when λ = 0.

m	Kuo[30]	Blasius[31]	Present results
0	0.8673	0.8673	0.8672779
1	1.1147	1.1152	1.1146882

Table 2.2: Computations showing the comparison of the values of $-\theta'(0)$ for different values of *m* when $\lambda = N_b = N_t = 0$.

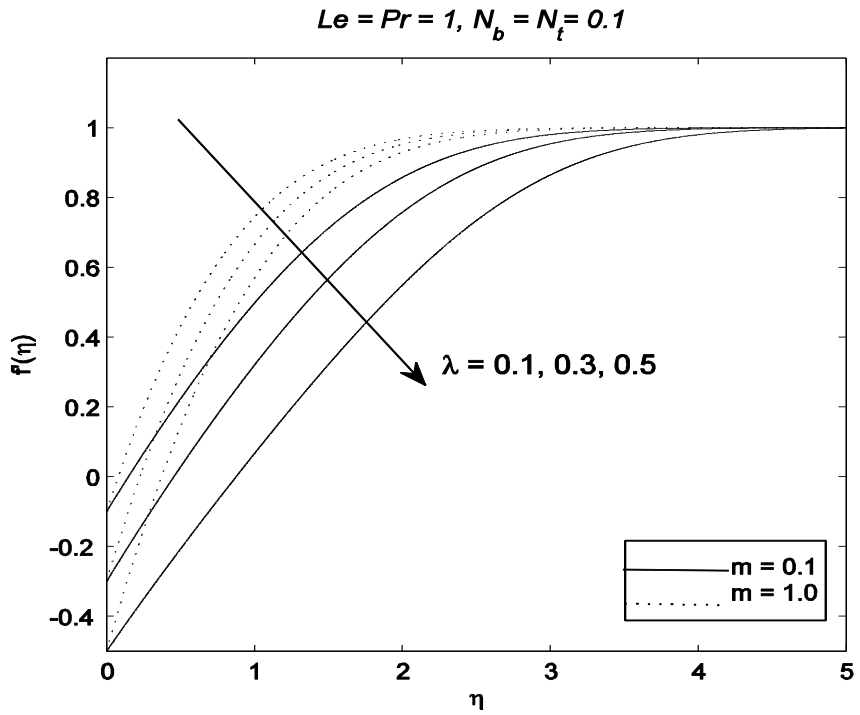

(a)

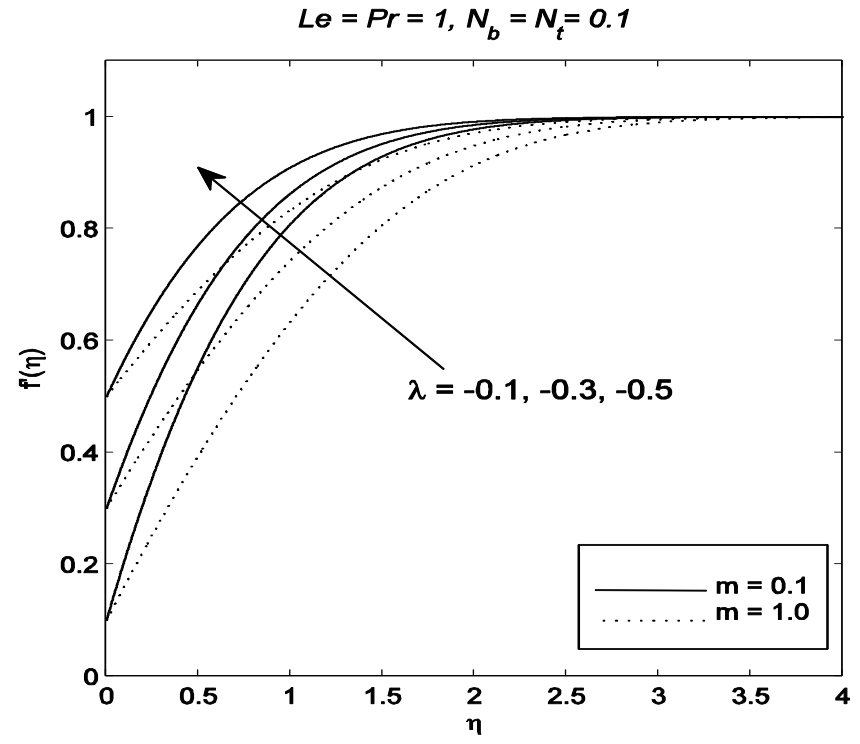

(b)

Fig. 2.1: Velocity profiles for the different values of m in case of (a) shrinking and (b) stretching wedge.

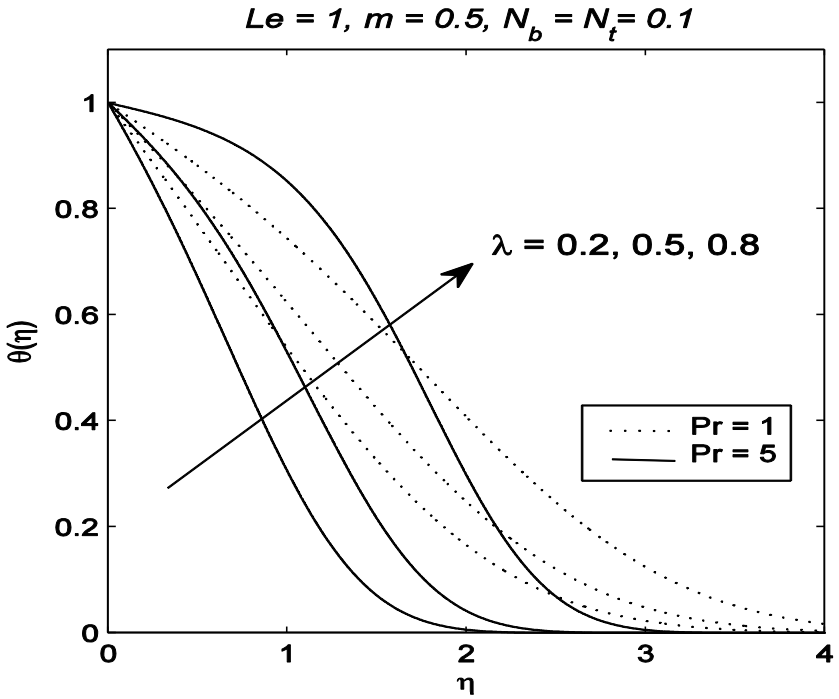

(a)

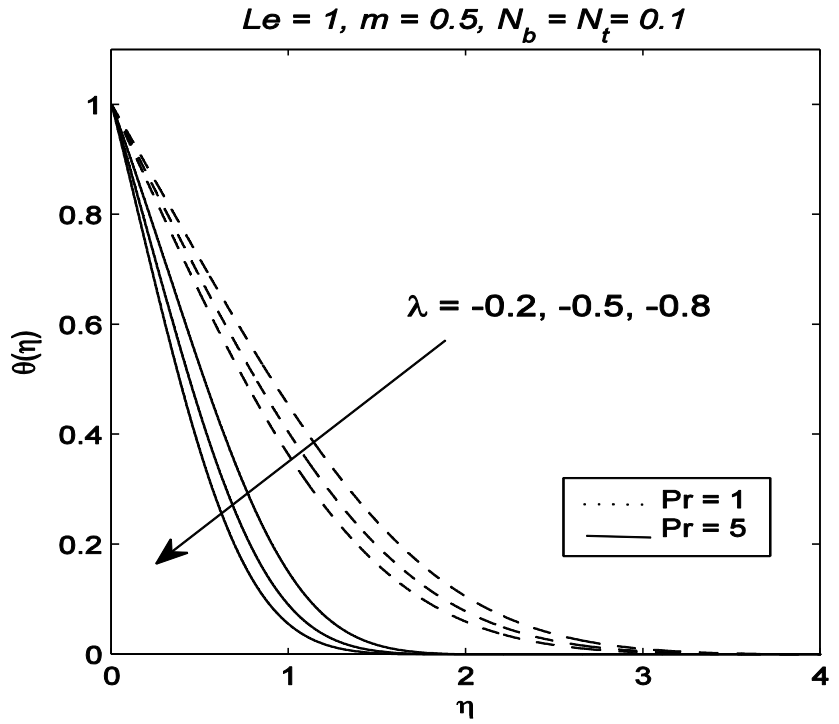

(b)

Fig. 2.2: The dimensionless temperature profiles for different values of Pr in the case of (a) shrinking and (b) stretching wedge.

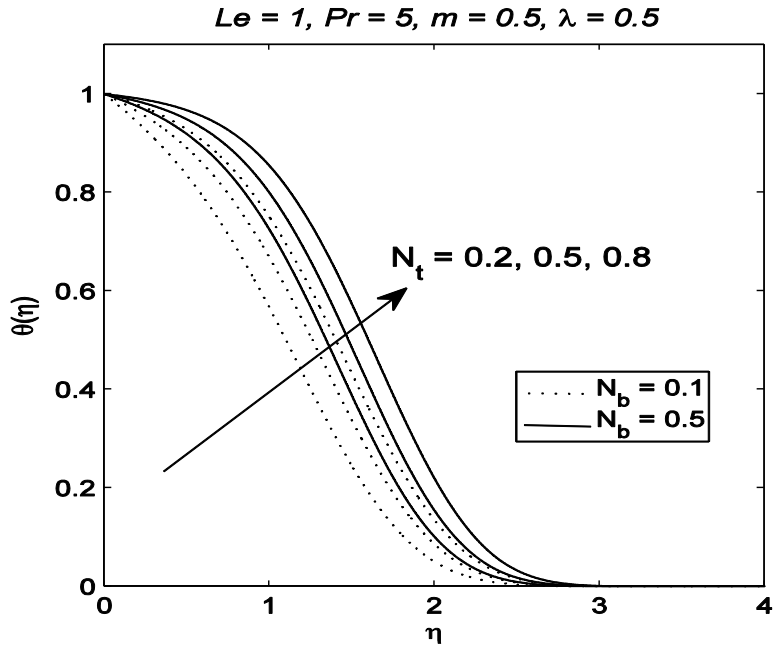

(a)

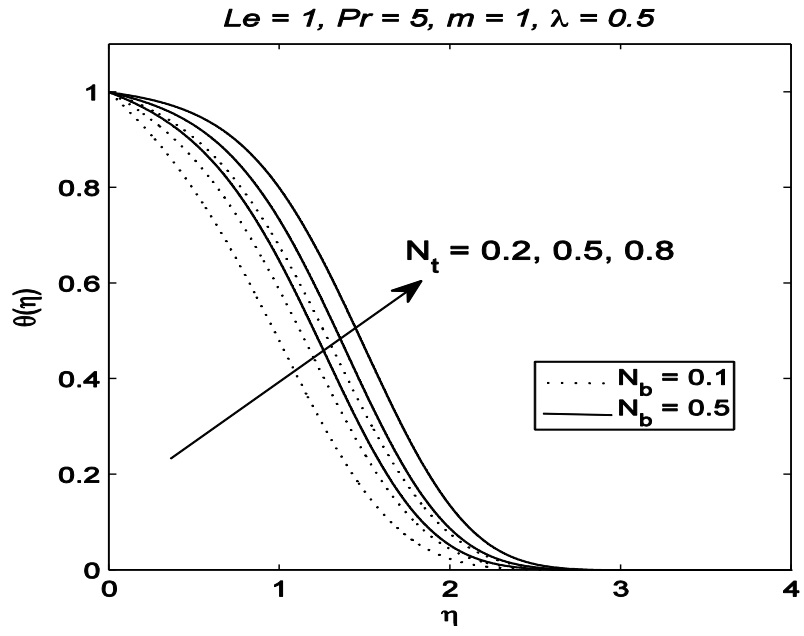

(b)

Fig. 2.3: Effect of nanofluid parameters on the dimensionless temperature along shrinking wedge for (a) $m = 1/2$ and (b) $m = 1$.

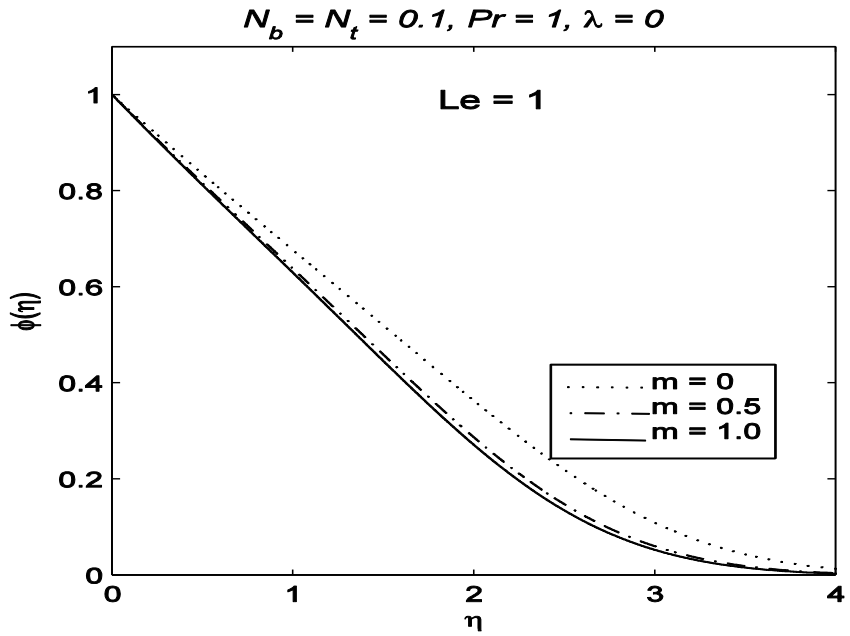

(a)

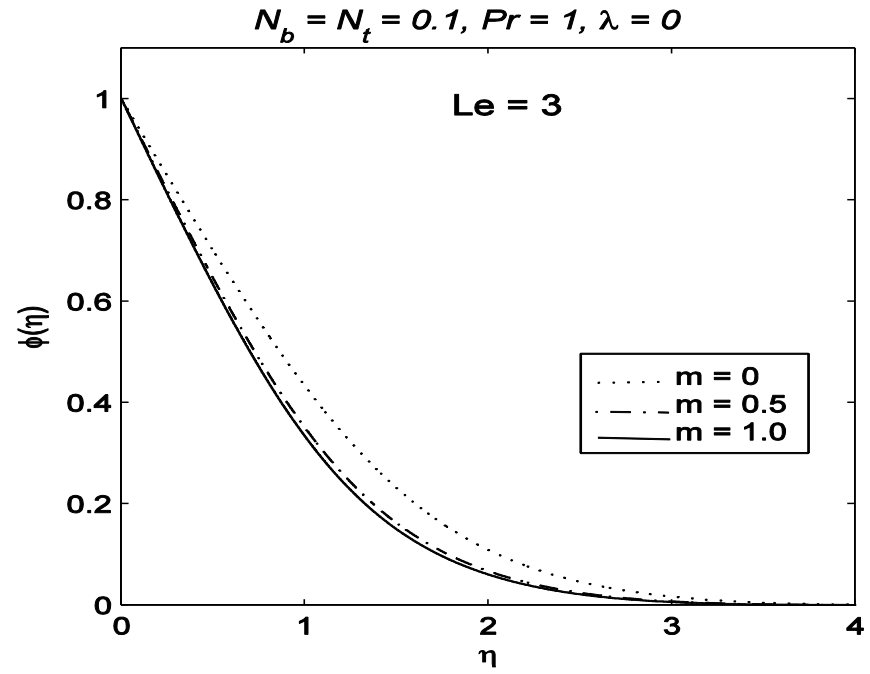

(b)

Fig. 2.4: Effects of wedge parameter on the dimensionless nanoparticle volume fraction profiles for different values of *m*.

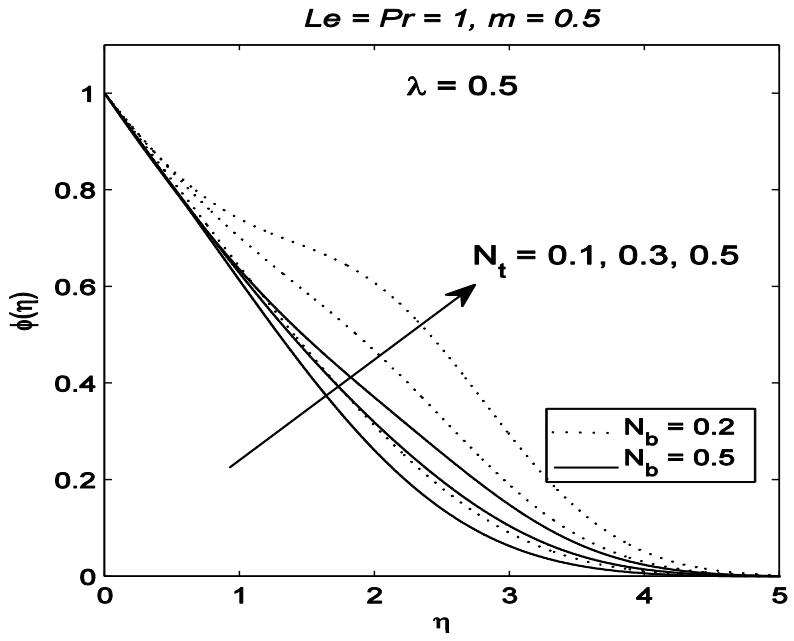

(a)

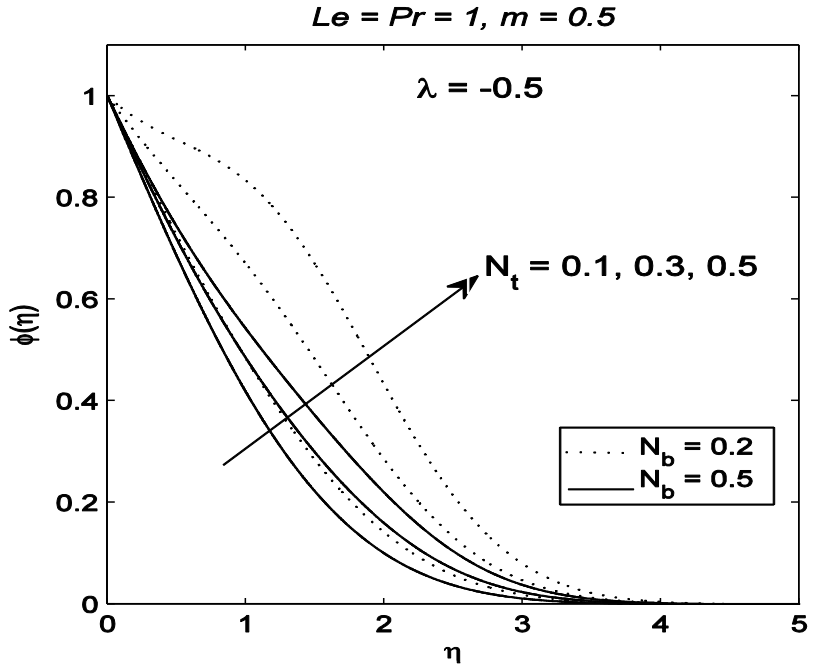

(b)

Fig. 2.5: Effects of nanofluid parameters on the dimensionless nanoparticle volume fraction for (a) shrinking wedge and (b) stretching wedge.

In Table 2.1 we compare our results for $f''(0)$ with those obtained by [27–29]. It can be seen that solutions are identical for all the considered values of the parameters. Table 2.2 compares the values of $-\theta'(0)$ obtained from Eqs. (2.2.8) and (2.2.9) for different values of m when $\lambda = N_b = N_t = 0$ with those of [30, 31]. The results of the two tables are proved accurate and correct by comparison with previous results.

Fig. 2.1(a) displays the velocity profiles for different values of m in the case of stretching wedge. Fig. 2.1(b) plots the corresponding results for shrinking wedge. The effect of wedge parameter *m* on velocity is found to increase/decrease upon increasing *m* in the case of stretching/shrinking wedge. The profiles approach the free stream condition faster for bigger values of *m.* This indicates that velocity is a decreasing function of *m.* The effect of Prandtl number on temperature distribution is shown in Fig 2.2. Prandtl number is defined as the ratio of momentum diffusivity to thermal diffusivity. A large Prandtl number fluid has relatively lower thermal diffusivity and hence thinner thermal boundary layer as can be observed from the Fig. 2.2. It is also found that temperature is an increasing function of λ.

The effects of Brownian motion and thermophoresis parameters on temperature are given in Fig. 2.3. An increase in the dimensionless temperature occurs with an increase in both Brownian motion and thermophoresis parameters. The variation of dimensionless nanoparticle volume fraction φ with wedge parameter *m* is given in Fig. 2.4(a) and 2.4(b). It is observed that an increase in wedge parameter decreases ϕ. This outcome is true for both theconsidered values of Lewis number. Fig. 2.5(a) and 2.5(b) depict the effects of nanofluid parameters on dimensionless nanoparticle volume fraction. An increase in Brownian motion and thermophoresis parameters corresponds to a decrease in nanoparticle volume fraction ϕ for both the values of λ.

Chapter 3

Falkner-Skan flow of nanofluids using passive control of nanoparticles at the wedge

This chapter extends the analysis of Chapter 2 by considering the revised model for nanofluids recently proposed by Kuzenstov and Nield [26]. This model requires nanoparticle volume fraction at the wall to be passively rather than actively controlled. Section 3.1 gives the mathematical formulation. The method of solution is given in Section 3.2. Finally the interpretation to the obtained results is given in Section 3.3.

3.1 Problem formulation

In the previous section, the boundary conditions for nanoparticle volume fraction analogous to those of the temperature were imposed. Here we revisit the problem of Chapter 2 by considering more meaningful boundary conditions for nanoparticle volume fraction suggested by Kuzenstov and Nield [26]. This condition requires that mass flux of nanoparticles at the wall is zero. The governing boundary layer equations with the boundary conditions are as under:

$$\frac{\partial u}{\partial x} + \frac{\partial v}{\partial y} = 0, \tag{3.1.1}$$

$$u\frac{\partial u}{\partial x} + v\frac{\partial u}{\partial y} = u_e\frac{du_e}{dx} + v\frac{\partial^2 u}{\partial y^2}, \tag{3.1.2}$$

$$u\frac{\partial T}{\partial x} + v\frac{\partial T}{\partial y} = \alpha\frac{\partial^2 T}{\partial y^2} + \tau\left[D_B\frac{\partial C}{\partial y}\frac{\partial T}{\partial y} + \frac{D_T}{T_\infty}\left(\frac{\partial T}{\partial y}\right)^2\right], \tag{3.1.3}$$

$$u\frac{\partial C}{\partial x} + v\frac{\partial C}{\partial y} = D_B\frac{\partial^2 C}{\partial y^2} + \frac{D_T}{T_\infty}\left(\frac{\partial^2 T}{\partial y^2}\right). \tag{3.1.4}$$

$$v = 0, \quad u = u_w(x) = -\lambda u_e(x), \quad T = T_w, \quad D_B\frac{\partial C}{\partial y} + \frac{D_T}{T_\infty}\frac{\partial T}{\partial y} = 0, \text{ at } y = 0,$$

$$u \to u_e(x), \qquad T \to T_\infty, \qquad C \to C_\infty \quad \text{as } y \to \infty. \tag{3.1.5}$$

where the variables appearing in above Eqs. (3.1.1) - (3.1.4) are defined in the previous chapter. Using the similarity transformations,

$$\eta = \left(\frac{(1+m)u_e}{2xv}\right)^{1/2} y, \quad \psi = \left(\frac{2u_e xv}{1+m}\right)^{\frac{1}{2}} f(\eta), \quad \theta(\eta) = \frac{T-T_\infty}{T_w-T_\infty}, \quad \phi(\eta) = \frac{C-C_\infty}{C_\infty}. \tag{3.1.6}$$

Continuity Eq. (3.1.1) is satisfied identically and Eqs. (3.1.2) - (3.1.5) become:

$$f''' + ff'' + \beta(1 - f'^2) = 0, \tag{3.1.7}$$

$$\frac{1}{Pr}\theta'' + f\theta' + N_b\theta'\phi' + N_t\theta'^2 = 0, \tag{3.1.8}$$

$$\phi'' + Lef\phi' + \frac{N_t}{N_b}\theta'' = 0, \tag{3.1.9}$$

$$f(0) = 0, \quad f'(0) = -\lambda, \quad \theta(0) = 1, \quad N_b\phi'(0) + N_t\theta'(0) = 0, \tag{3.1.10}$$

$$f'(\infty) = 1, \quad \theta(\infty) = 0, \quad \phi(\infty) = 0.$$

The parameters appearing in Eqs. (3.1.7)-(3.1.9) are defined as below:

$$\beta = \frac{2m}{1+m}, \qquad Pr = \frac{v}{\alpha}, \qquad Le = \frac{v}{D_B}, \qquad N_b = \frac{(\rho c)_p D_B (C_\infty)}{(\rho c)_f v}, \tag{3.1.11}$$

$$N_t = \frac{(\rho c)_p D_T (T_w - T_\infty)}{(\rho c)_f T_\infty v}.$$

Here the quantities of practical interest are the skin friction coefficient C_f and local Nusselt number Nu defined as below:

$$C_f = \frac{\tau_w}{\rho {u_w}^2},$$

$$Nu = \frac{x q_w}{k(T_W - T_\infty)},$$

using dimensionless variables (3.1.6), one obtains:

$$f''(0) = Re_x^{-1/2} C_f,$$

$$Nur = Re_x^{-1/2} Nu = -\theta'(0),$$

where $Re_x = \frac{u_w(x)x}{v}$ is the local Reynold's number and $q_w = -k\left(\frac{\partial T}{\partial y}\right)_{y=0}$ is the wall heat flux.

3.2 Results and discussion

We apply Keller-box method for solving Eqs. (3.1.7) - (3.1.9) numerically. The method is briefly explained in the previous chapter.

N_t	$\mathrm{Nur} = (-\theta'(0))$				
	m = 0.2	m = 0.4	m = 0.6	m = 0.8	m = 1.0
0.1	0.4857065	0.5109619	0.5250507	0.5341987	0.5406644
0.2	0.4833909	0.5083805	0.5223170	0.5313641	0.5377574
0.3	0.4810624	0.5057855	0.5195692	0.5285152	0.5348360
0.4	0.4787210	0.5031769	0.5168075	0.5256521	0.5319003
0.5	0.4763667	0.5005547	0.5140318	0.5227749	0.5289503
0.6	0.4739994	0.4979190	0.5112423	0.5198837	0.5259861
0.7	0.4716193	0.4952697	0.5084390	0.5169784	0.5230079
0.8	0.4692262	0.4926070	0.5056219	0.5140593	0.5200156
0.9	0.4668204	0.4899309	0.5027912	0.5111263	0.5170095
1.0	0.4644017	0.4872415	0.4999469	0.5081797	0.5139896

Table 3.1: Computations showing the reduced Nusselt number $(-\theta'(0))$ for different values of m and N_t when Le = Pr = 1.0, $\lambda = N_b = 0.1$.

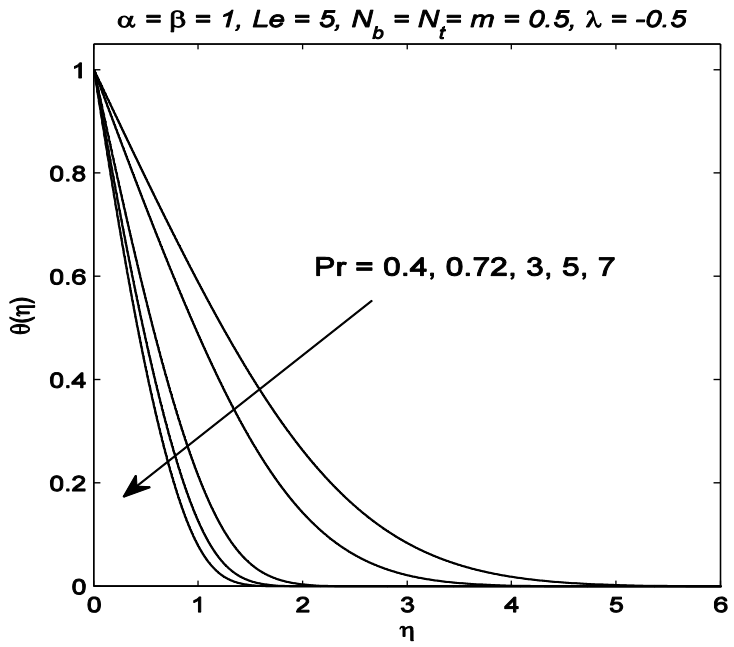

Fig. 3.1: Effect of Pr on the temperature profiles for stretching wedge.

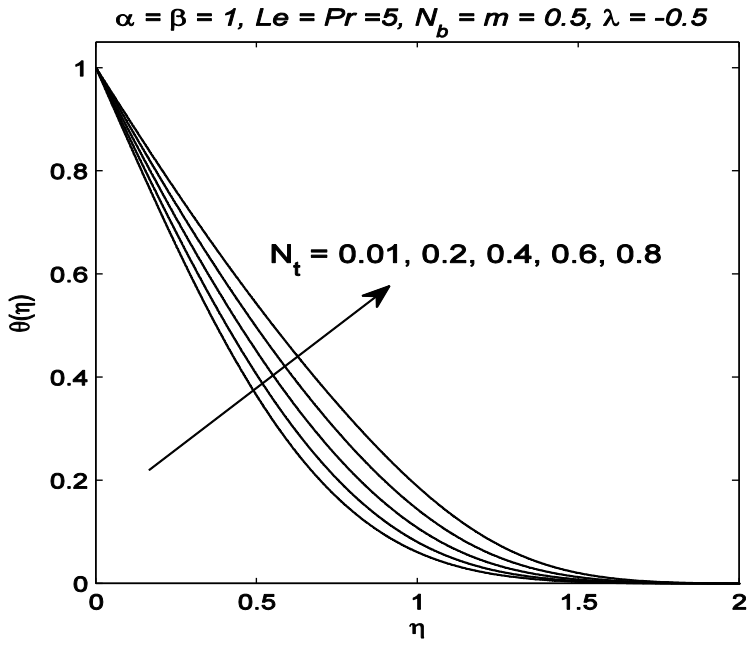

Fig. 3.2: Effect of Nt on the temperature profile for stretching wedge.

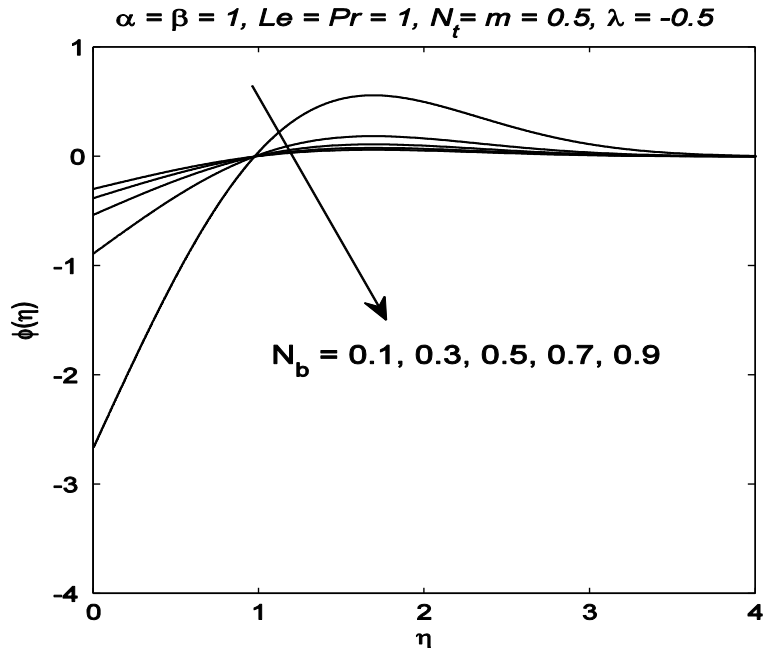

Fig. 3.3: Effect of N_b on the dimensionless nanoparticle volume fraction for shrinking wedge.

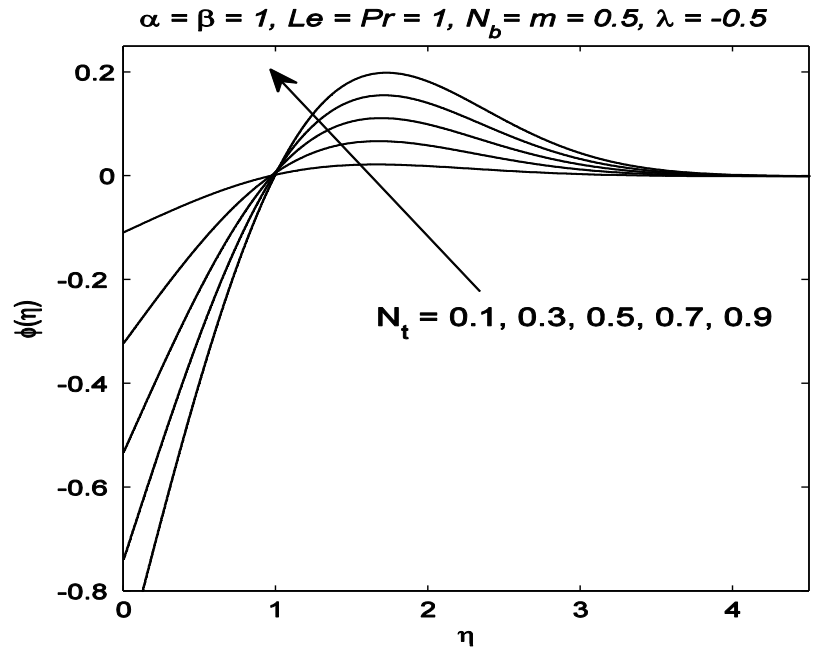

Fig. 3.4: Effect of N_t on the dimensionless nanoparticle volume fraction for stretching wedge.

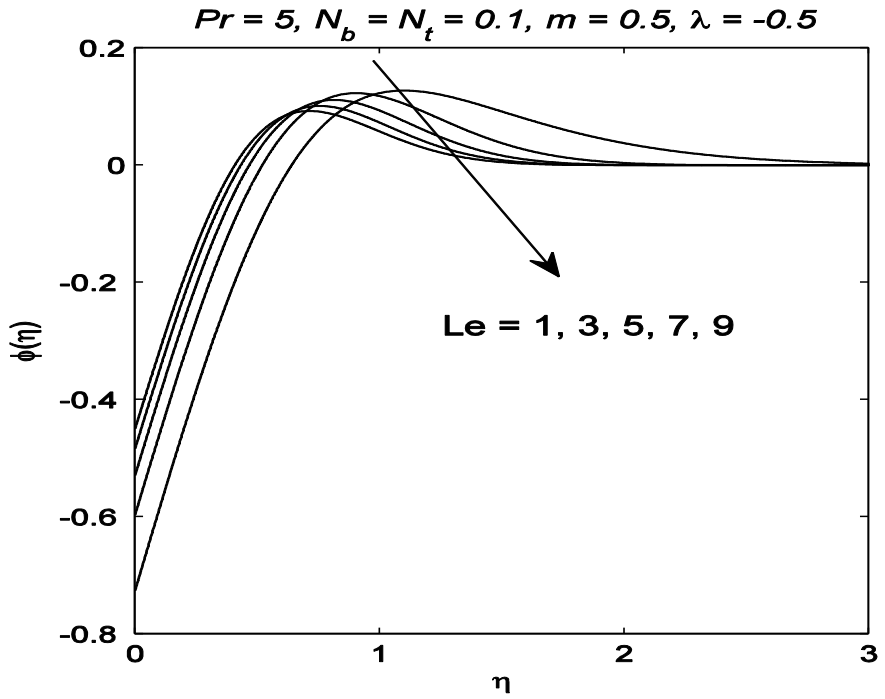

Fig. 3.5: Effect of *Le* on the dimensionless nanoparticle volume fraction for stretching wedge.

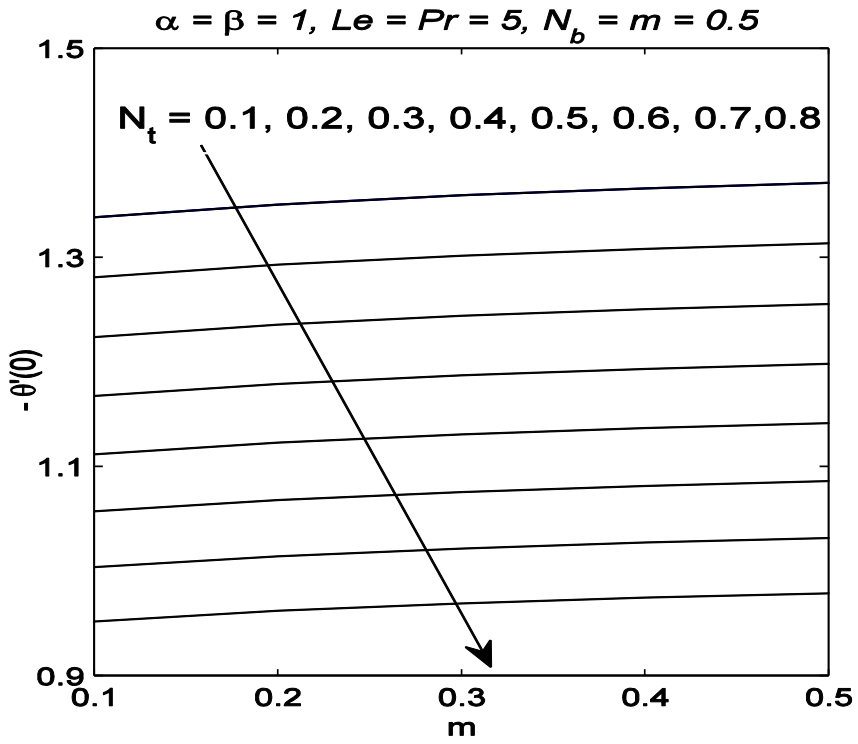

Fig. 3.6: Effect of N_t on the reduced Nusselt number.

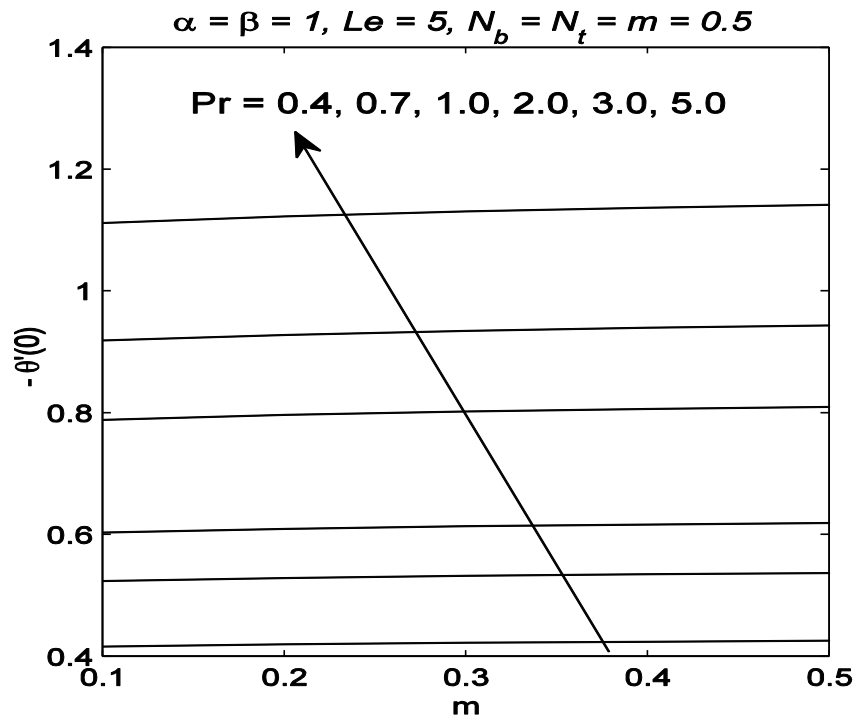

Fig. 3.7: Effect of *Pr* on the reduced Nusselt number

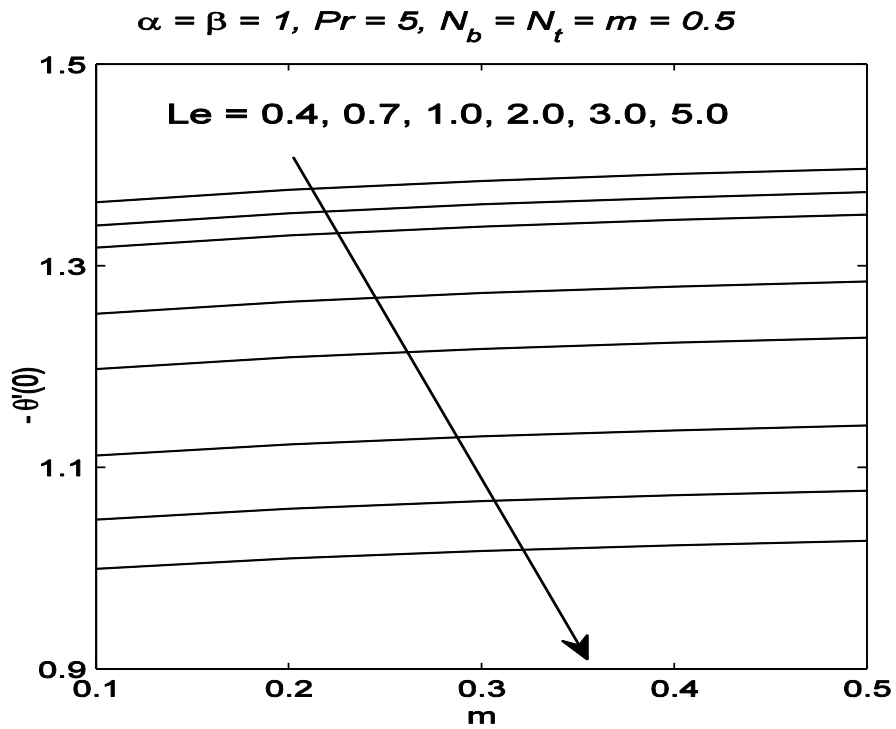

Fig. 3.8: Effect of Le on the reduced Nusselt number.

Table 3.1 provides a sample of our results for the reduced Nusselt number Nur corresponding to different parametric values. This table indicates that Nur is a decreasing function of dimensionless parameter N_t. However, reduced Nusselt number increases when m is increased.

Fig. 3.1 indicates the behavior of Prandtl number Pr on the thermal boundary layer. A higher Prandtal number fluid possesses weaker thermal conductivity. Therefore an increase in Pr corresponds to a decrease in conduction which gives shorter penetration depth of temperature θ. This outcome can be visualized in Fig. 3.1 where profiles tend to their free stream condition much faster as Pr is increased. The decrease in the thermal boundary layer thickness is compensated with a larger magnitude of local Nusselt number. Thermophoresis parameter (N_t) and Brownian motion parameter (N_b) are used for controlling the heat transfer rates in nanofluids. Fig. 3.2 gives the temperature variation in the thermal boundary layer by varying N_t. As N_t is increased, the temperature and thermal boundary layer thickness increases. Fig. 3.3 shows the impact of N_b on dimensionless nanoparticle volume fraction ϕ in the case of stretching wedge ($\lambda = -0.5$). It is seen that nanoparticle volume fraction decreases with the increase in Brownian motion. The effect of N_t on dimensionless nanoparticle volume fraction ϕ is shown in Fig. 3.4 in the case of stretching wedge ($\lambda = -0.5$). An increase in N_t shifts nanoparticles from hot stretching sheet towards cold ambient fluids. This leads to larger penetration depth of ϕ as demonstrated in Fig. 3.4. Fig. 3.5 shows that Lewis number has a significant effect on concentration distribution. A higher Lewis number fluid has a lower Brownian diffusion coefficient D_B which results in shorter penetration depth for ϕ. Fig. 3.6 indicates that reduced Nusselt number is a decreasing function of thermophoresis parameter N_t. On the other hand it has a direct relationship with m. Fig. 3.7 shows that the heat transfer rate from the wedge is bigger for larger Prandtl number nanofluid. It is clear from Fig. 3.8 that reduced Nusselt number is inversely proportional to the Lewis number Le.

Chapter 4

Conclusions

Steady boundary layer flow past a moving wedge in a water based nanofluid is studied numerically using an implicit finite-difference method known as Keller-box method. The imposed condition requires that mass flux of nanoparticles at the wall is zero. Effect of all governing parameters on the dimensionless velocity, temperature, and nanoparticle volume fraction are investigated and presented graphically. The key points of this work are as under:

1) Dimensionless velocity at the surface increases/decreases with stretching/shrinking parameters.
2) Dimensionless temperature and thermal boundary layer thickness increase with an increase in thermophoresis parameter.
3) Brownian motion has a negligible impact on the temperature profile.
4) An increase in Prandtl number causes a decrease in temperature which results in decrease of thermal boundary layer thickness.
5) An increase in thermophoresis parameter results in increase of dimensionless nanoparticle volume fraction.
6) Dimensionless nanoparticle volume fraction decreases with an increase in Lewis number.
7) An increase in Prandtl number results in reduction of boundary layer thickness, thus increasing the reduced Nusselt number.
8) The reduced Nusselt number decreases resulting in increase in surface temperature by increasing Lewis number.

References

[1] V. M. Falkner and S. W. Skan, Some approximate solutions of the boundary-layer equations, Philosophical Mag. 12 (1931) 865–896.

[2] S. D. Harris, D. B. Ingham and I.Pop, Unsteady heat transfer in impulsive Falkner-Skan flows, Euo. J. Mech. 21 (2002) 447-468.

[3] A. Pantokratoras, The Falkner-Skan flow with constant wall temperature and variable viscosity, Int. J. Therm. Sci. 45 (2006) 378–389.

[4] B. L. Kuo, Heat transfer analysis for the Falkner-Skan wedge flow by the differential transformation method, Int. J. Heat Mass Trans. 48 (2005) 5036-5046.

[5] T. Fang, Ji. Zhang, An exact analytical solution of the Falkner-Skan equation with mass transfer and wall stretching, Int. J. Non-Linear Mech. 43 (2008) 1000-1006.

[6] H. Bararnia, N.Haghparast and A.Barari, Flow analysis for the Fakner-Skan wedge flow, Current sci. 103 (2012) 2-25.

[7] N. Riley, P. D. Weidman, Multiple solutions of the Falkner-Skan equation for low past a stretching boundary, SIAM J. App. Math. 49 (1989) 1350–1358.

[8] A. Ishak, R. Nazar, and I. Pop, Falkner-Skan equation for low past a moving wedge with suction or injection, J. App. Math. & Comp. 25 (2007) 67–83.

[9] S.U.S. Choi, Enhancing thermal conductivity of fluids with nanoparticles, Dev. App. Non-Newtonian Flows, 66 (1995) 99-105.

[10] J. Buongiorno, Convective transport in nanofluids, ASME J. Heat Trans. 128 (2006) 240-250.

[11] D. A. Nield, A. V. Kuznetsov, The Cheng–Minkowycz problem for natural convective boundary-layer flow in a porous medium saturated by a nanofluid, Int. J. Heat Mass Trans. 52 (2009) 5792–5795.

[12] A. V. Kuznetsov, D. A. Nield, Natural convective boundary-layer flow of a nanofluid past a vertical plate, Int. J. Therm. Sci. 49 (2010) 243–247.

[13] S. Ahmad, I. Pop, Mixed convection boundary layer flow from a vertical fat plate embedded in a porous medium filled with nanofluids, Int. Comm. Heat Mass Trans. 37 (2010) 987-991.

[14] Bachok, A. Ishak, R. Nazar, I. Pop, Flow and heat transfer at a general three-dimensional stagnation point in a nanofluid, Physica B 405 (2010) 4914-4918.

[15] W. A. Khan, I. Pop, Boundary-layer flow of a nanofluid past a stretching sheet, Int. J. Heat Mass Trans. 53 (2010) 2477–2483.

[16] A. V. Kuznetsov, D. A. Nield, Double-diffusive natural convective boundary-layer flow of a nanofluid past a vertical plate, Int. J. Therm. Sci. 50 (2011) 712–717.

[17] D. A. Nield, A. V. Kuznetsov, The Cheng–Minkowycz problem for the double-diffusive natural convective boundary layer flow in a porous medium saturated by a nanofluid, Int. J. Heat Mass Trans. 54 (2011) 374–378.

[18] O. D. Makinde, A. Aziz, Boundary layer flow of a nanofluid past a stretching sheet with a convective boundary condition. Int. J. Therm. Sci. 50 (2011) 1326–1332.

[19] A. Aziz, W.A. Khan, Natural convective boundary layer flow of a nanofluid past a convectively heated vertical plate, Int. J. Therm. Sci. 52 (2012) 83–90.

[20] N. Bachok, A. Ishak and I. Pop, Boundary layer flow over a moving surface in nanofluid with suction or injection, Acta Mech. Sin. 28 (2012) 34–40.

[21] P. Rana, R. Bhargava, Flow and heat transfer of a nanofluid over a nonlinearly stretching sheet, Commun. Nonlinear Sci. Num. Sim. 17 (2012) 212–226.

[22] N. Bachok, A. Ishak and I. Pop, Boundary layer stagnation-point flow and heat transfer over an exponentially stretching/shrinking sheet in a nanofluid, Int. J. Heat Mass Trans. 55 (2012) 8122–8128.

[23] K. Zaimi, A. Ishak and I. Pop, Boundary layer flow and heat transfer past a permeable shrinking sheet in a nanofluid with radiation effect, Adv. Mech. Eng. 340354 (2012) 1–7.

[24] M. M. Rahman, I. A. Eltayeb, Radiative heat transfer in a hydromagnetic nanofluid past a non-linear stretching surface with convective boundary condition, Meccanica 48, (2013) 601–615.

[25] W. A. Khan, I. Pop, Boundary layer flow past a wedge moving in a nanofluid, J.Appl. Math. Prob. Eng. (2013) doi:10.1155/2013/637825.

[26] A. V. Kuznetsov, D. A. Nield, Natural convective boundary-layer flow of a nanofluid past a vertical plate: A revised model, Int. J. Therm. Sci. 77 (2014) 126–129.

[27] K. A. Yih, Uniform suction/blowing effect on forced convection about a wedge: uniform heat flux, Acta Mech. 128 (1998) 173–181.

[28] N. A. Yacob, A. Ishak, I. Pop, Falkner-Skan problem for a static or moving wedge in nanoluids, Int. J. Therm. Sci. 50 (2011) 133–139.

[29] F. M. White, Viscous Fluid Flow, McGraw-Hill, New York, NY, USA, 2nd edition, (1991).

[30] B. L. Kuo, Heat transfer analysis for the Falkner-Skan wedge flow by the differential transformation method, Int. J. Heat Mass Trans. 48 (2005) 5036–5046.

[31] H. Blasius, Grenzschichten in Flussigkeiten mit kleiner Rei-bung, Zentralblatt Math. Phy. 56 (1908) 1–37.